PAPER

Check for updates

Heparin sodium enriched gelatin/polycaprolactone based multi-layer nanofibrous scaffold for accelerated wound healing in diabetes

Madhukiran R. Dhondale, [ID] Manjit Manjit, [ID] Abhishek Jha, [ID] Manish Kumar, [ID] Kanchan Bharti, [ID] Dinesh Kumar and Brahmeshwar Mishra [ID] *

Multilayered nanofibrous scaffolds (MNSs) obtained by electrospinning have gained widespread attention owing to their control over the delivery of drugs. However, polymer and drug solubility issues in common solvent systems still limit their applications. The present work employed acetic acid : water : ethyl acetate (4 : 4 : 2 v/v/v) as a common solvent system for dissolving gelatin and heparin sodium (HS). A GL 20% w/v solution showing optimum viscosity and conductivity, and high encapsulation (89.2 ± 2.13%) was selected. Additionally, TPGS-1000 incorporated in GL reduced the surface tension for better electrospinning and additional free-radical scavenging activity (~6 fold of blank nanofibers). The central layer was surrounded by upper and lower PCL–GL layers to control the release of the hydrophilic drug (HS). The electrospun PCL : GL layer sustained the release for ~24 hours. The developed multilayered nanofibrous scaffolds showed accelerated wound healing in a diabetic rat model. Histological analysis of the wound confirmed the accelerated re-epithelialization and reduced inflammatory response. Laser Doppler flowmetry further showed a significant improvement in the blood flow at the wound site at day 14 and day 21, revealing neo-vascularization. Therefore, the developed multilayered nanofibrous scaffolds provided a plausible method for fabricating regenerative scaffolds for drug delivery and diabetic wound healing.

1. Introduction

Diabetic foot ulcer (DFU) is a severe consequence of untreated diabetes due to peripheral neuropathy, along with other deficiencies such as an impaired angiogenic response, reduced collagen deposition and matrix metalloproteases (MMP) assisted remodelling.[1] Treatment approaches include various topical formulations such as hydrogels, creams, sponges, *etc*. However, the use of traditional topical formulations is found to be unable to completely heal diabetic wounds. Currently, numerous formulation-based approaches are being explored among which electrospun nanofibers are gaining prominence due to their widespread applicability in tissue engineering. Nanofibers, owing to their properties such as high surface-to-volume ratio and interconnected porous structure, provide a suitable environment for cell attachment and growth. Electrospun nanofibrous scaffolds mimic the native extracellular matrix (ECM) for tissue regeneration[2] and

wound healing.[3,4] Nanofibrous scaffolds can be modified to control the release of their load by altering the polymer type and concentration.[5] Numerous modifications have been reported in the electrospinning instrumentation and procedures to fabricate various types of nanofibers such as composite, core–sheath, and Janus nanofibers.

Simple blend electrospinning, which involves the preparation of a homogenous solution of the polymer and drug in a suitable solvent followed by electrospinning, is the most basic and common method to fabricate nanofibers.[6] In this method, combination of hydrophilic and hydrophobic polymers can be used to control the drug release profile as well as to improve its cytocompatibility.[7] Similarly, to achieve the controlled release of the drug and impart dual functionality to the nanofibers, further modifications were explored by researchers which led to the advent of coaxial electrospinning using a co-axial needle.[8] This method enabled researchers to use two different solutions and drugs (dual loading) for electrospinning to form core–sheath nanofibers.[9,10] Further modifications such as the use of triaxial needles for electrospinning is also well documented, wherein tri-layered nanofibers can be obtained with different drugs and polymers loaded in each eccentric layer of the nanofiber.[11–13] However, the method suffers disadvantages due to the risk of needle clogging and

Department of Pharmaceutical Engineering and Technology, Indian Institute of Technology (BHU) Varanasi, Uttar Pradesh, India. E-mail: bmishra.phe@itbhu.ac.in, madhukirandr.rs.phe22@itbhu.ac.in, manjit.rs.phe20@itbhu.ac.in, abhishekjha.phe17@itbhu.ac.in, manishkumar.rs.phe19@itbhu.ac.in, Kanchan.bharti.rs.phe18@itbhu.ac.in, dinesh.phe@itbhu.ac.in

requires specialized spinnerets. Other techniques such as surface modification/functionalization, cross-linking of nano-fibers, and formation of bead-on-a-string morphology nano-fibers can also modify the drug release profiles.[14–16] The above-mentioned methods basically involve modifications in the spinnerets for electrospinning or involve the use of additional chemical crosslinkers. Also, the use of multiple solutions for electrospinning complicates the process and poses significant scalability issues.[14]

The layer-by-layer technique is another nanofiber preparation technique used for preparing nanofibrous scaffolds. Herein, multiple layered nanofibers of varying thickness can be fabricated to modify the release kinetics. Additionally, this technique is quite simple compared to other electrospinning techniques.[5] Therefore, the current work involves the design of multilayered nanofibrous scaffold (MNS) using polymer blends in order to modulate the release of payload for regulated and accelerated wound healing.

Poly-(ε-caprolactone) (PCL) is an FDA approved biodegradable and biocompatible polymer with extended drug release kinetics and excellent mechanical strength with applications in tissue engineering.[17–19] However, PCL cannot be used on its own due to its high hydrophobicity, which can interfere with the wound healing process.[3,19] Hence it is used in combination with a hydrophilic polymer such as gelatin/collagen. Gelatin (GL), an abundantly available hydrophilic natural polymer with excellent biodegradability, biocompatibility, non-immunogenicity, and non-toxicity.[20] GL exhibits excellent activity in promoting wound healing, mimics ECM, and promotes cell adhesion and tissue regeneration. Therefore, a PCL and GL blend was proposed for modulating the release of payload from MNS. Herein, heparin sodium (HS), a glycosaminoglycan was loaded into nanofibers due to its capability of healing chronic wounds such as diabetic foot ulcers.[21–23] Sufficient literature references support the role of heparin in promoting wound healing through its anti-inflammatory activity,[24] neoangiogenesis,[25] reepithelialization,[26] myofibroblast formation and wound closure activities.[27]

Therefore, we propose loading HS into GL nanofibers as a central drug reservoir surrounded by hydrophobic layers of PCL–GL nanofibers of varying thickness to control the release of HS. However, incorporating HS into GL nanofibers is very challenging due to its solubility issues and it has not been previously reported in the literature. Therefore, a suitable solvent system was proposed for the fabrication of HS loaded GL nanofibers. In addition to HS, vitamin E TPGS was also incorporated in the GL layer which is well known for facilitating prompt healing of wounds owing to its antioxidant properties. The fabricated MNSs were evaluated for morphology, hydrophilicity, *in vitro* drug release, and wound healing activity in a diabetic rat model.

2. Materials and methods

2.1. Materials

Unfractionated heparin sodium was obtained from Emcure Pharmaceuticals, Pune. TPGS-1000 and PCL (average M_n

80 000) were purchased from Sigma Aldrich, USA. Gelatin Type-A was purchased from HiMedia Laboratories Pvt. Ltd. Solvents such as acetic acid, formic acid, ethyl acetate, and ethanol were purchased from Spectrochem Pvt. Ltd, Mumbai. Toluidine blue-O was procured from SRL Pvt. Ltd., India. All other reagents used were of analytical grade.

2.2. Fabrication of multilayered nanofibrous scaffolds (MNSs)

For fabrication of the central GL nanofiber core (inner layer-IL), gelatin type-A (10, 12.5, 15, 20 and 25% w/v) in the selected solvent system of acetic acid : water : ethyl acetate in the ratio 4 : 4 : 2 v/v/v was used for electrospinning. For the drug loaded nanofibers, HS (1% w/v) and TPGS-1000 (1% w/v) dissolved in the solvent system prior to GL were used for electrospinning. For fabrication of the outer PCL/GL sheath (outer layers-OL), PCL/GL (50 : 50, 60 : 40, and 70 : 30 w/w) dissolved in an acetic acid–formic acid mixture (7 : 3 v/v) was used for fabrication of the outer layer. The total polymer concentration was 15% w/v and the mixture was magnetically stirred for 4–5 h to obtain a clear solution for electrospinning of the outer layer. The multi-layered nanofibrous scaffold was prepared by a layer-by-layer technique where the PCL/GL layer was fabricated as the first layer (OL). The GL central layer was fabricated over OL over which again the PCL/GL layer was fabricated to give a sandwich model of MNS. The inner layer (IL) of the GL nanofiber loaded with HS and TPGS-1000 sandwiched between outer layers (OL) of PCL–GL were of different thicknesses. Thickness was defined based on the volume of the electrospun OL solution. The volume of IL was kept constant at 0.8 mL while OL volumes were varied (0.1 mL, 0.2 ml, and 0.3 mL). The nano-fibers were dried under vacuum for 24 hours post spinning to remove the residual solvents. The total nine formulations were fabricated as per the composition listed in Table 1.

2.3. Measurement of the electrospinning solution properties

Viscosity. Viscosity of various polymer concentrations was measured using the Brookfield DV-III Ultra Programmable Rheometer using spindle-62 at 100 rpm and 25 °C.[28] All the measurements were conducted in triplicate.

Conductivity. The conductivity of the polymeric solution was carried out using a portable conductivity meter. For this, the

Table 1 Composition of different nanofiber formulations

Formulation	OL composition (GL : PCL ratio)	Volume of outer layers (mL)	Volume of inner layer (mL)
F_1	50 : 50	0.1	0.8
F_2		0.2	0.8
F_3		0.3	0.8
F_4	40 : 60	0.1	0.8
F_5		0.2	0.8
F_6		0.3	0.8
F_7	30 : 70	0.1	0.8
F_8		0.2	0.8
F_9		0.3	0.8

probe of the conductivity meter was dipped into the polymeric solution until the readings stabilized and the recording was done in triplicate.

Electrospinnability. The electrospinning operations were carried out using the in-house assembled electrospinning unit in the Department of Pharmaceutical Engineering and Technology, IIT(BHU), Varanasi, India. The prepared solutions were loaded in a 5 mL syringe with a 22G needle. The needle was connected to a high DC voltage output device (Genvolt Pvt. Ltd, India) and a voltage of 10–16 kV was supplied. During fabrication, the flow rate of the IL and OL solution was varied between 0.2 and 0.5 mL h^{-1} using a syringe pump (Genvolt Pvt. Ltd). The collector was placed 10 cm away from the needle tip.

2.4. Characterization of nanofibers

The morphology (fiber diameter and appearance) of the GL nanofibers with/without HS and PCL–gel nanofibers were evaluated using scanning electron microscopy (SEM) (ZEISS EVO 18 Research, USA). SEM images were used to measure the fiber diameter and porosity using Catymage and ImageJ software, respectively. For the diameter measurements, at least 100 individual nanofibers were analysed. The HS loading in gel nanofibers was also confirmed by scanning electron microscopy-energy dispersive X-ray (SEM-EDX) analysis.

For measurement of the entrapment efficiency (EE), a nanofibrous mat of IL (20% w/v GL with 1% w/v of HS) was electrospun. From the resulting nanofibrous mat, a specified quantity (in terms of weight) was cut and dissolved in deionized water. The solution was suitably diluted and the heparin concentration was measured by a colorimetric method utilizing toluidine blue-O (TBO) dye. The absorbance of the solution was measured using a UV-Visible spectrophotometer (UV-1800, Shimadzu, Japan) at 530 nm.[29] The % EE was calculated using eqn (1).

$$\text{Entrapment efficiency}(\%) = \frac{\text{Amount of drug in sample (mg)}}{\text{Theoretical amount of drug loading in the sample (mg)}} \times 100 \tag{1}$$

The contact angle was measured using a Drop Shape Analyzer (DSA25S, KRUSS, Germany) to determine the hydrophilicity of the fabricated nanofibers. Briefly, a 2 μL drop of water was dropped on the nanofiber surface from a syringe and a static image was taken to determine the angle. The lower the angle, the higher the hydrophilicity of the nanofibers will be.

2.5. *In vitro* drug release study

In vitro drug release profiling of prepared nanofibers was done in phosphate buffer (pH 7.4). A known weight of the MNS mat of dimension (1 × 1 cm^2) was cut and transferred to 1 mL phosphate buffer in a sealed vial. The vials were immersed in a water bath shaker running at 50 strokes per minute at 37 °C

± 1 °C. At specified time points, the whole portion of buffer was withdrawn and replaced with an equivalent volume of fresh buffer to maintain the sink condition.[3] Experiments were run in triplicate per sample and cumulative drug release was determined and plotted.

2.6. Solid-state characterization

Fourier Transform Infrared (FTIR) spectroscopy (Shimadzu 8400 S) was done to explore the possible chemical interaction between the drug and polymer(s), the drug stability, as well as effect of electrospinning on the functional groups of the drug loaded in the formulation. The FTIR spectra of the drug alone, the gelatin and the nanofibers were recorded in range of 400 to 4000 cm^{-1} with 2 cm^{-1} resolution by scanning the KBr pellet.

Powder X-ray diffraction (PXRD) was employed to determine the possible changes in crystalline property of the drug encapsulated in nanofiber film. The individual drug, polymer(s) and nanofibers were examined by a benchtop X-ray diffractometer (MiniFlex 600, Rigaku, Japan). The samples were scanned in a rotating holder at a scan rate of 4° min^{-1} (over a 2θ range of 5° to 60°).

2.7. Mechanical strength testing

The prepared nanofibers, GL (20% w/v) NF, PCL : GL (60 : 40) NF and multilayered nanofibrous scaffold (GL–TPGS–HS NF) were subjected to tensile strength testing using an Instron universal testing machine. The samples were connected to the jaws and stretched under constant strain of 5 mm min^{-1}.

2.8. The free-radical scavenging efficacy of the nanofibers

The free radical scavenging activity of the developed nanofibrous mat was measured using a 2,2-diphenyl-1-picrylhydrazyl (DPPH) assay. Briefly, a known quantity of nanofiber was cut and incubated in a methanolic solution of DPPH (3 mL; 100 μM concentration). The resultant sample was kept in dark conditions at ambient temperature (25 °C ± 2 °C). After incubation for 30 min, the absorbance was measured at 517 nm by a UV-Vis spectrophotometer to obtain A_{sample}.[3] Similarly, the readings were taken for DPPH solutions ($A_{\text{DPPH pure}}$) without the nanofiber sample. DPPH scavenging efficacies were determined by eqn (2).

$$\text{DPPH scavenging efficacies} (\%) = \left(\frac{A_{\text{DPPH pure}} - A_{\text{sample}}}{A_{\text{DPPH pure}}} \right) \times 100 \tag{2}$$

2.9. *In vivo* wound healing activity in diabetic rats

The optimized nanofiber mat was evaluated for its *in vivo* wound healing efficacy in diabetic rats. All animal procedures were performed after obtaining approval of the Institutional Animal Ethics Committee of Indian Institute of Technology (Banaras Hindu University) Varanasi, India (IIT(BHU)/IAEC/2023/013), registered under the Committee for the Purpose of Control and Supervision of Experiments on Animals (CPCSEA), India. All experiments were carried out as per the (ARRIVE)

2.0 guidelines. A total of 24 healthy adult Sprague-Dawley rats of both sex, each weighing around 200–250 g, were selected. The rats were treated with an intraperitoneal streptozotocin (45 mg kg^{-1}) injection in 0.1 M citrate buffer (pH 4.5). The blood glucose levels of all the rats were monitored using a glucometer (Accu-check, Germany) for 7 days after the injection. Rats with pre-prandial blood glucose concentration above 360 mg dL^{-1} for a minimum of 5 days were considered as diabetic.[30] The animals were anaesthetized using an intraperitoneal injection of ketamine (80 mg kg^{-1}) and xylazine (10 mg kg^{-1}). The dorsum of the rats was shaved and decontaminated with 70% iso-propyl alcohol. The skin near the dorsum was excised to create a full thickness circular wound with an approximate diameter of 1 cm. The animals were randomly divided into four groups ($n = 6$) as the control (saline), blank nanofiber (PCL–Gel nanofiber), nanofiber formulation (PCL–Gel–HS–TPGS nanofiber), and marketed product (silver sulfadiazine cream). The wound closure rate was determined to check the efficacy of the nanofibrous mat in wound healing. For this, pictures of the wound were taken on days 7, 14, and 21. The wound area was measured using ImageJ software and the percentage wound area was graphically plotted for each group.

For histological examination on day 14 and day 21, hematoxylin and eosin (H&E) staining was conducted. For this, granulation tissue was extracted from the healed area of the rats. The tissue sections (~4 μm thick) were taken and stained using hematoxylin–eosin (H&E). The stained tissue sections were viewed under microscope to assess the histological condition of the healed tissue and wound healing in different treatment groups were compared.

The laser Doppler flowmetry was carried out to measure the blood flow at the wound site of the animals on days 14 and day 21. The rats were anaesthetised as mentioned in section 2.5.6 and the images of the wounded area were captured using the laser Doppler instrument. The blood flow in terms of blood perfusion units (BPU) in the region of interest (ROI) was measured with OMEGAZONE OZ-2 software.

2.10. Statistical analysis

Wherever applicable, studies were conducted in triplicate and the values are reported as mean ± standard deviation (SD). Statistical analysis was carried out by two-way analysis of variance (ANOVA) and significance was shown at $p < 0.05$.

3. Results and discussion

A preliminary study was conducted to select an appropriate solvent system for dissolving both HS and GL in a single solvent system. The selection of solvent system was crucial as HS is insoluble in most commonly used electrospinnable solvents such as hexafluoroisopropanol (HFIP) and trifluoroethanol (TFE). The limited solubility of HS required a suitable solvent system suitable for electrospinning HS with GL. In this regard, a water based solvent system was proposed. When a higher proportion of water was used as a co-solvent, a higher

voltage was required for electrospinning to give defect free nanofibers, due to the high surface tension of water (72 dyne cm^{-1}). Also, pure water as solvent was unsuitable as it formed a gel-like consistency at higher gelatin concentrations. Therefore, acetic acid and ethyl acetate (surface tension – 27 dyne cm^{-1} and 24 dyne cm^{-1}, respectively) were added to reduce the surface tension and aid in dissolving GL by reducing the pH.[31] Furthermore, a reduction in the water amount in the solvent system resulted in precipitation of HS from the solvent system. Hence, water was required in the specified ratio in a solvent system to achieve the proper electrospinning of HS and GL. To mitigate these issues, acetic acid : water : ethyl acetate (4 : 4 : 2 v/v/v) was selected as the solvent system for electrospinning the central GL–NFs layer. The proposed solvent system facilitated electrospinning at a higher concentration (>20% w/v) of GL.

Additionally, solution viscosity and conductivity can influence the electrospinnability of GL nanofibers as sub-optimal viscosity and conductivity leads to bead defects.[19] Therefore, the viscosity and conductivity of various GL solutions were measured (Fig. 1). The GL concentration was found to play a key role in solution viscosity, conductivity, nanofiber diameter and morphology. At 10% w/v GL concentration, the solution viscosity was too low (27.6 ± 1.2 cps) to form a Taylor cone. Additionally, 10% w/v GL exhibited a conductivity of 1688.33 ± 3.05 μS cm^{-1} and showed no regular fiber formation due to very low concentration. At a slightly higher concentration (12.5% w/v), the unstable Taylor cone was observed, as a result, the fibers were not continuous. The conductivity and viscosity values of the solution were 2004.3 ± 4.0 μS cm^{-1} and 52.4 ± 3.0 cps, respectively. The fibers formed were very thin as observed by naked eye during electrospinning. The SEM analysis revealed a defective nanofiber with numerous beaded structures and non-uniform fibers (64.9 ± 26.3 nm). Furthermore, 15% w/v GL concentration increased the conductivity and viscosity to 2212.2 ± 9.53 μS cm^{-1} and 81.6 ± 1.2 cps, and a relatively stable Taylor cone formed, which ensured continuous nanofibers. However, bead defects were still observed and fibers of diameter 105.3 ± 37.5 nm were obtained. The lower polymer concentration was observed to have an extremely low viscosity giving instabilities during electrospinning. The Rayleigh instability due to insufficient solution viscosity was responsible for the beaded morphology of the electrospun nanofibers.[32] Hence, the concentration was further increased to 20% w/v, which resulted in bead-free, smooth, and continuous nanofibers. The fiber diameter also increased to 214.2 ± 58.7 nm due to the higher GL concentration. The conductivity and viscosity were observed to be 2414 ± 9.5 μS cm^{-1} and 142 ± 0.6 cps, respectively. A further increase in GL concentration to 25% w/v GL resulted in fused nanofibers of about 275.5 ± 59.3 nm, probably due to the very high viscosity (292.1 ± 1.2 cps) and incomplete solvent evaporation.

For further studies, fabrication of HS loaded GL nanofibers and PCL : GL nanofibers was done using 20% w/v GL solution due to its feasibility in producing smooth defect-free nanofibers. GL nanofibers loaded with HS (inner layer) and
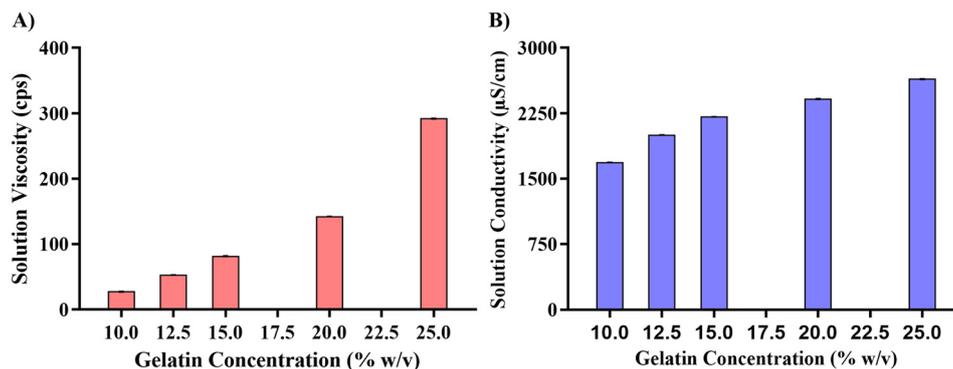
Fig. 1 (A) Viscosity and (B) conductivity of GL solutions.

PCL : GL nanofibers (outer layer) of different compositions were electrospun and analysed by SEM to study their morphology. Upon addition of 1% w/v TPGS-1000 and HS to 20% w/v GL solution, the fiber diameter reduced to 116.07 ± 16.64 nm. This can be attributed to the increase in hydrophilicity and surface tension lowering activity of TPGS-1000.[3] No defects were seen in the drug loaded nanofibers. For the fabrication of the PCL : GL layer, a previously optimized formula in our lab was used.[3] The final polymer concentration was kept at 15% w/v in the acetic acid : formic acid mixture (7 : 3 v/v), and the ratio of PCL : GL was varied. Three combinations 50 : 50, 60 : 40 and 70 : 30 w/w were tried based on the release profile and hydrophilicity. The morphology and size distribution of the prepared PCL : GL nanofibers was in agreement with the previous study by Ajmal *et al.*[3] The SEM micrographs and fiber diameter distribution curves are shown in Fig. 2. The SEM images were processed in the ImageJ software to calculate the porosity of the prepared outer layer (PCL–GL) and inner layer (GL–TPGS-100–HS). The scaffold with higher surface area and porosity favours the cell attachment and allows for easy exchange of gases between the tissue and environment.[33] A porous network allows uniform distribution of cells while seeding and provides sufficient space for the accommodation of cells. The prepared nanofibers exhibited nanofiber diameter and porosity of 116.07 nm ± 16.62 nm and 85.86%, 170.56 nm ± 24.4 nm and 77.92%, 115.72 nm ± 21.37 nm and 82.11%, 89.91 nm ± 17.74 nm and 78.77% for GL–TPGS-HS, PCL : GL (50 : 50), PCL : GL (60 : 40) and PCL : GL (70 : 30), respectively. The nanofibers exhibited a porosity of >75% suggesting them to be an excellent platform for cell growth. The ideal porosity of scaffolds should usually be within the range of 60–90%.[34] Therefore, fabricated nanofibers were ideal and acceptable for the desired application.

Another advantage of electrospinning for nanofiber fabrication is high drug entrapment efficiency (~90%).[35] This trend is observed only under the conditions of complete miscibility of drug and polymer, non-volatile nature of the drug, and optimum concentration of the drug. Using the solvent system of acetic acid : water : ethyl acetate 4 : 4 : 2 (v/v/v), the complete dissolution of both HS and GL was possible. Hence, a high

entrapment efficiency of 89.2 ± 2.13% was observed for the prepared nanofiber formulation. The remaining drug (~10%) could be considered as process loss during electrospinning. Thus, our study suggested blend electrospinning of a highly water-soluble drug (HS) with GL/TPGS using a cheap and non-toxic aqueous-based solvent system to obtain nanofibers with a high payload. The blend electrospinning using acetic acid : water : ethyl acetate 4 : 4 : 2 (v/v/v) as the solvent system was successful in fabricating smooth nanofibers with high entrapment of HS, as confirmed by the SEM-EDX analysis. Fig. 3A shows the image of nanofiber and its corresponding elemental composition (of the selected area in the image). The identification of elements specific to HS such as sodium and sulphur confirms the entrapment of HS in the nanofibrous matrix.

The drug release studies were performed for formulations with an outer layer (PCL : GL nanofibers) of different polymer ratio and thicknesses (Table 1). The plot between the cumulative amount of drug release *vs.* time for the prepared formulations is shown in Fig. 3B. The ratio of 50 : 50 for PCL : GL (50 : 50) showed a burst release, attributed to hydrophilic gelatin responsible for faster dissolution of nanofibrous mat and thus drug release. The PCL ratio used here was not found to be sufficient to sustain the release for longer duration, releasing around 50% of the drug within 1.5 h from all three formulations (F1–F3). Followed by an initial burst release, the formulations followed a controlled release profile for about 12 h. F3 with highest thickness of PCL : GL 50 : 50 (w/w) was able to provide release at a slower rate. This suggested that PCL, though hydrophobic in nature is required at a higher ratio to sustain the drug release and reduce burst effect from nanofibrous matrix.

To further study the effect of PCL concentration in the outer layer on drug release, the ratio was increased to 60 : 40 (w/w) for PCL : GL. The ratio found to control the release of HS from the formulations (F4–F6) was probably due to the combined effect of gelatin swelling controlled release and hydrophobic barrier provided by PCL.[36] Comparatively, F6 showed a higher control over the release of entrapped HS for about 18 hours. On increasing the ratio to 70 : 30 (w/w) for PCL : GL, more pronounced control over drug release was observed. The
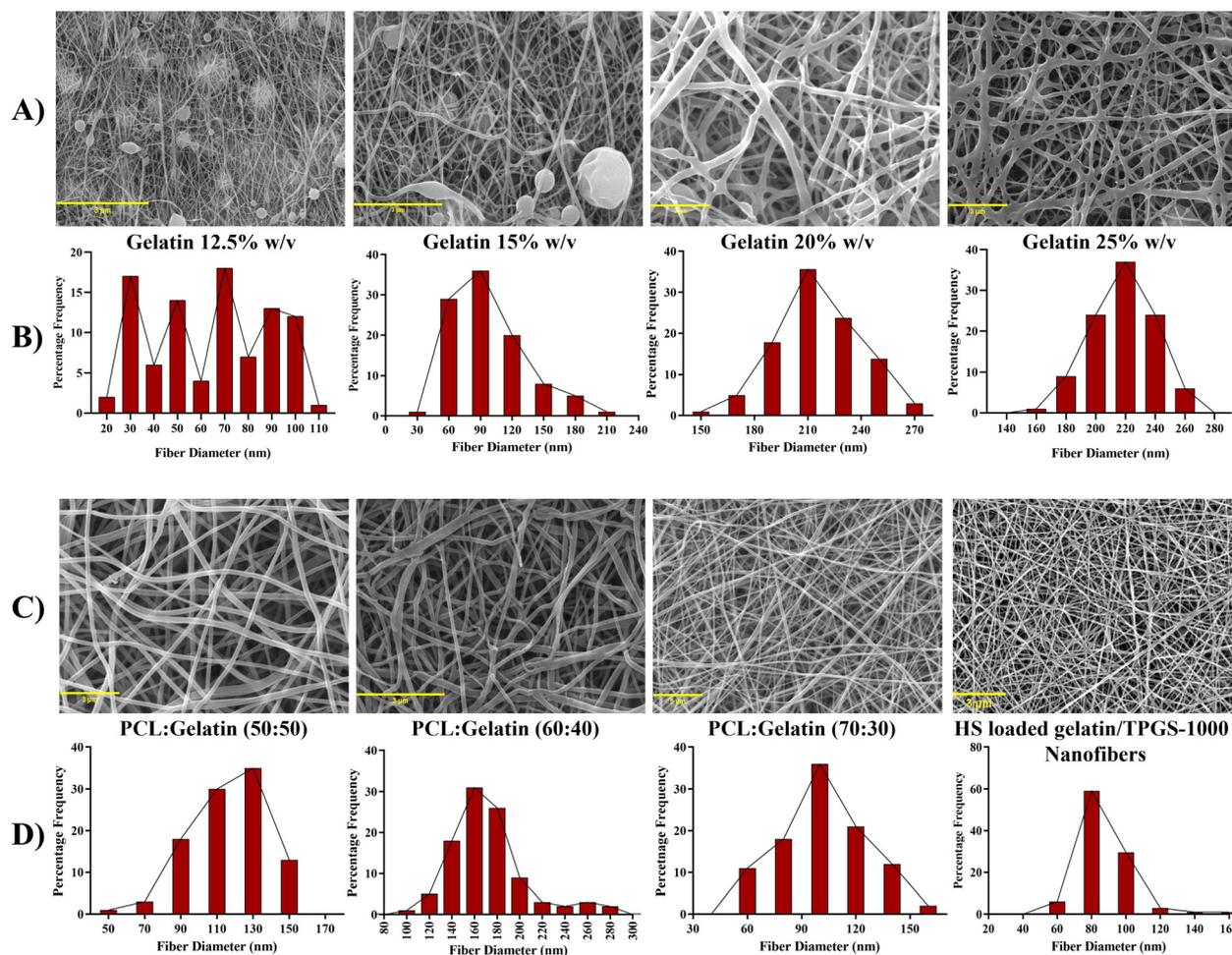
Fig. 2 (A) & (C) SEM micrographs of nanofibers, (B) & (D) fiber diameter distribution of the respective nanofibers (scale bar represents the size of 3 μm).

burst effect was significantly controlled, except in F7 with the lowest outer layer thickness. In addition, Formulation F9 with a similar outer layer thickness as F6 and higher PCL amount was found to further prolong the release of HS for ~24 hours. The prolonged release was due to higher hydrophobicity (high PCL in outer layer) and swelling of GL, which increased the traverse route for free drug from the matrix. Hence, the above ratio was used as the outer layer for fabrication of MLNs mats. Herein, the polymer (PCL) concentration and thickness was found to play a major role in controlling the drug release. The increase in both can have better control over the release of the encapsulated drug. Further research should be carried out to assess the impact of molecular weight of PCL and GL on the release rate of the encapsulated drugs.

The surface property of scaffolds is another useful property of nanofibers that determines adhesion and proliferation of fibroblasts on the nanofibrous membrane. A hydrophilic surface augments the cell adhesion and proliferation, while a hydrophobic surface shows poor cell adhesion. The hydrophilicity of the nanofiber surface was examined by measuring the contact angle between a sessile drop of water and membrane surface, and the results are shown in Fig. 3D. The contact angle of the nanofiber layer with the highest PCL concentration was in the acceptable range (~83°) which indicates that all the prepared formulations are sufficiently hydrophilic to support the attachment and growth of fibroblasts and promote healing of diabetic wounds. The contact angle between the nanofiber and sessile water drop reduced as a function of PCL concentration reduction. The results were in-line with the previously reported findings.[35] The nanofiber with the 50 : 50 w/w PCL ratio showed the highest hydrophilicity (contact angle of ~49 °C with a water droplet). The results were in agreement with the burst drug release effect observed in F1, F2, and F3 equipped with an outer layer with high wettability.

Fourier-transform infra-red (FTIR) spectroscopic analysis was carried out to explore the effect of electrospinning on the functional groups of drug and polymers. Since the drug was in the GL nanofibers, an overlay FTIR spectrum of HS, GL nanofiber, TPGS-1000, physical mixture, and formulation (GL–TPGS–HS NF) was presented (Fig. 4A). The characteristic peaks of HS appeared at 1618.33 cm^{-1} (COOH-stretching), 3464.2 cm^{-1} (a broad and intense peak indicating OH-stretch-
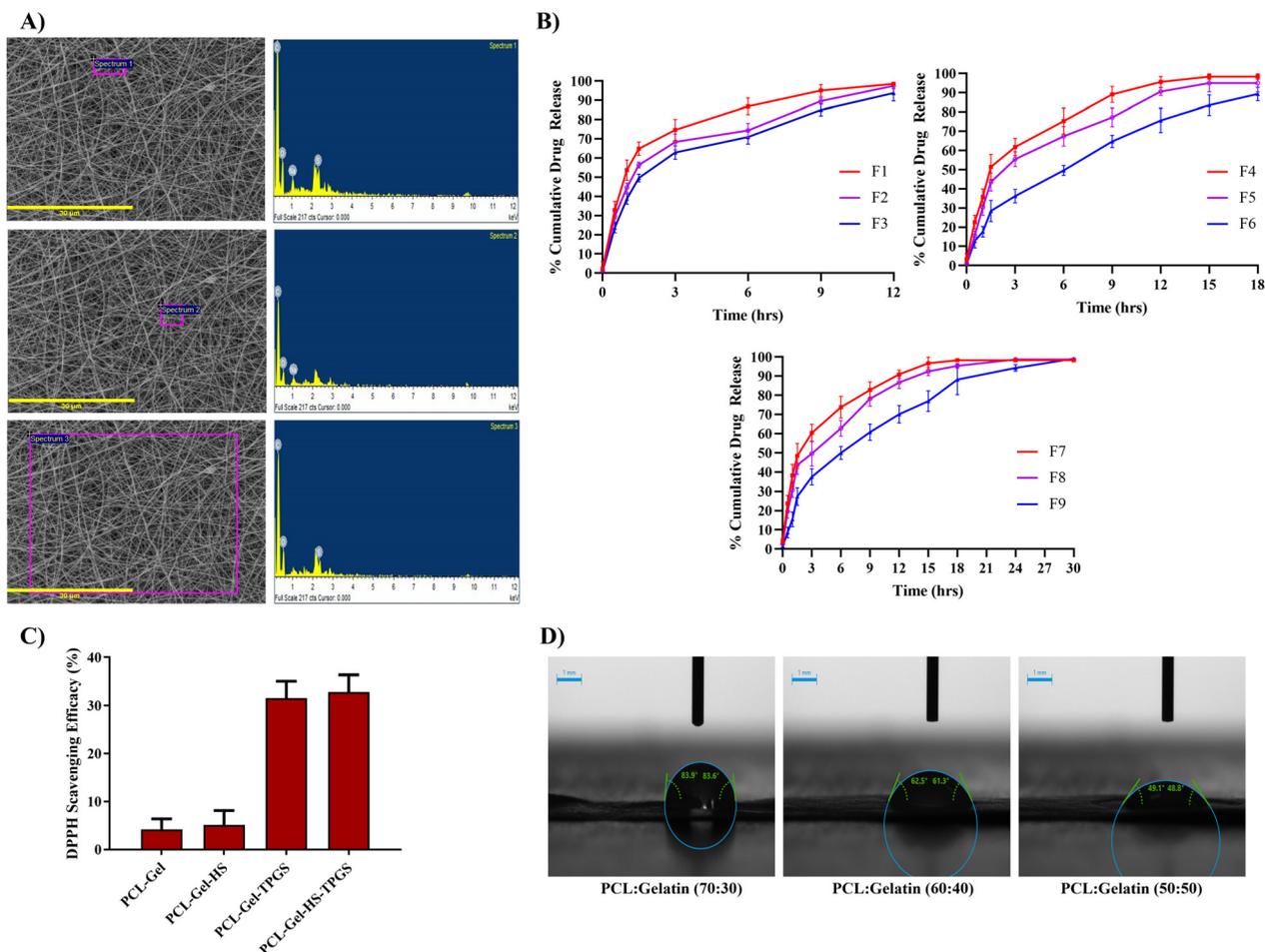
Fig. 3 (A) SEM–EDX analysis of HS loaded GL nanofibers, (B) *in vitro* drug release profiles of different nanofiber formulations, (C) *in vitro* anti-oxidant assay of nanofibers, and (D) images of contact angle (at 3 s) of different PCL : GL nanofibers.

ing), 2945.4 cm^{-1} (NH-stretching), 1232.55 cm^{-1} and 1026.16 cm^{-1} (S=O asymmetric stretching and bending, respectively), and 941.29 cm^{-1} and 815.92 cm^{-1} (C–O–S asymmetric and symmetric stretching, respectively). Gelatin also contains similar functional groups to that of HS (except S=O and C–O–S). The nanofiber formulation (GL–TPGS–HS NF) exhibited no major shifts in the peak positions, thus confirming the compatibility of drug and polymers. The results also showed that the electrospinning process and organic solvents (acetic acid and ethyl acetate) exhibited no deteriorated effect on heparin sodium, confirming the structural stability of heparin sodium post electrospinning. The powder X-ray diffraction (PXRD) overlay spectrum confirmed the amorphous nature of nanofibers post electrospinning with GL and TPGS-1000 (Fig. 4B). This was attributed to encapsulation of drug in hydrophilic TGPS–GL nanofibers.

The free-radical scavenging efficacies of nanofibers were established by the DPPH reduction method. The scaffold possessed scavenging activity probably due to TPGS-1000, a derivative of the natural anti-oxidant, vitamin-E. The multi-layered nanofibrous membrane containing TPGS-1000 with or without

HS displayed free radical scavenging property compared to nanofibers without TPGS-1000 (Fig. 3C). TPGS-1000 equipped nanofibers displayed ~6 fold higher free radical scavenging efficacy than nanofibers without TPGS-1000. Since reactive oxygen species play a major role in pathogenesis of DFU, control over ROS can have significant effects in the treatment of DFU. Thus TPGS-1000 incorporated into nanofibers as an surfactant[37] served as a potent anti-oxidant tool to overcome free radicals burden at the wound site in diabetic patients. The final nanofiber formulation (GL–TPGS–HS NF) showed tensile strength of 2.513 MPa. Pure gelatin nanofibers lack sufficient mechanical strength (tensile strength of 0.554 MPa) and hence addition of PCL in the scaffold resulted in an improvement in the tensile strength of the nanofibers (tensile strength of 2.285 MPa). Our results agree with the reported studies as well.[38] The stress strain curves are shown in Fig. 4C. Elongation (%) and tensile strength (MPa) results are given in Table 2.

The *in vivo* efficacy of the nanofibrous membrane was checked for its wound healing activity in the full thickness diabetic wound model (Fig. 5A). The formulation (F6) was chosen for wound healing studies considering its drug release profile
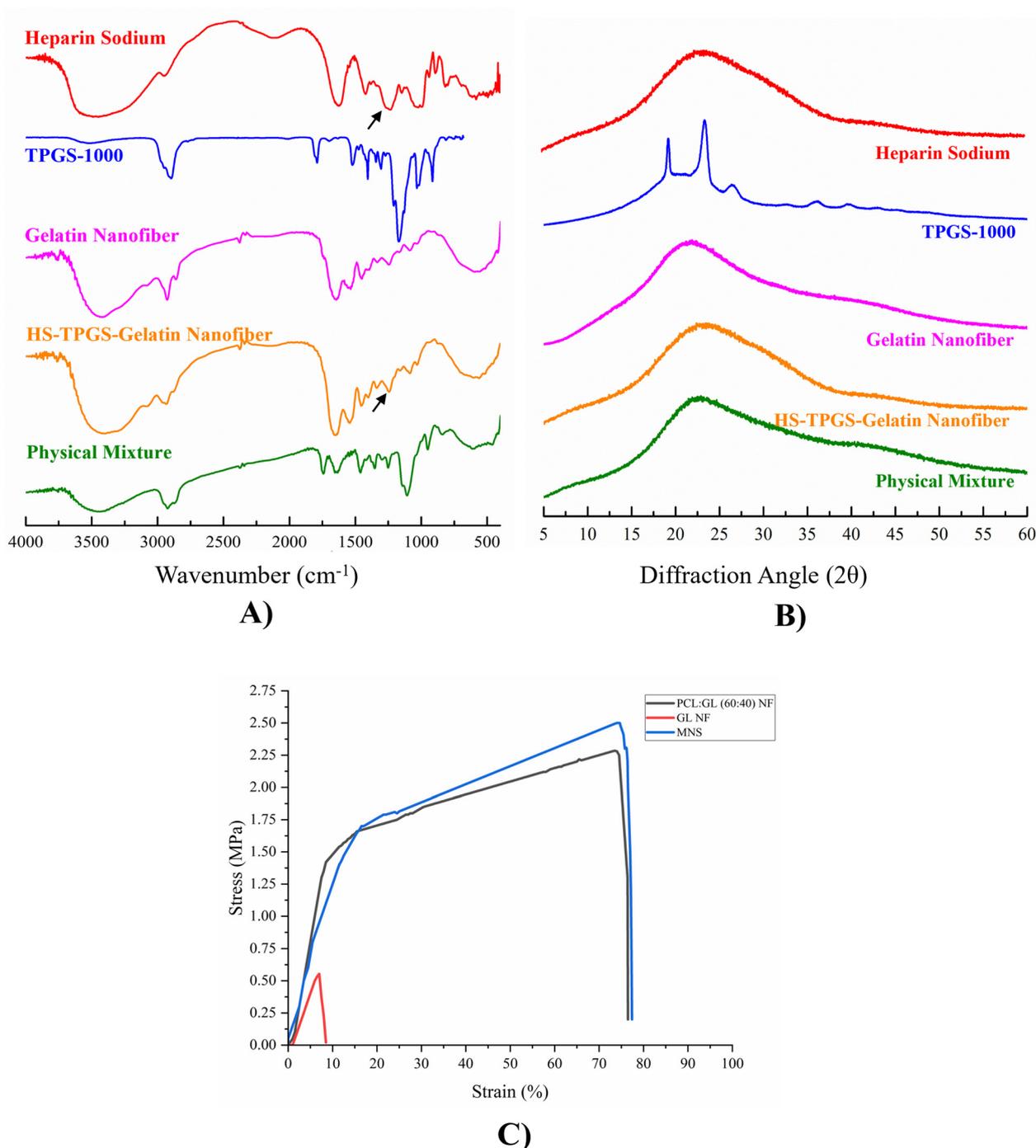
Fig. 4 Overlay spectra of (A) FTIR & (B) PXRD. (C) Stress−strain curves of the prepared nanofibers.

and water contact angle (hydrophilicity). The hydrophilic nanofibrous mats allow fibroblast cell attachment, thereby promoting wound healing. All treatment groups showed no signs of wound infection, death, or bleeding except the control group, which showed visible signs of weight loss and inflammation. The prepared nanofibers showed good attachment to the wound when applied. The nanofiber formulation (F6) treated group exhibited significant improvement in wound closure

compared to the control (Fig. 5B). The nanofiber treated group showed a significant difference in wound healing on days 14 and 21 when compared to blank nanofiber ($p < 0.05$ on both days 14 and 21) and marketed cream ($p < 0.01$ and $p < 0.05$ on days 14 and 21, respectively) treated groups. The accelerated wound healing for the nanofiber formulation treated group can be attributed to the combined effects of HS, gelatin and TPGS-1000, which resulted in suppression of inflammation,

Table 2 Mechanical strength of the prepared nanofibers

	Elongation (%)	Tensile strength (MPa)
GL NF	7%	0.554
PCL : GL (60 : 40) NF	73.5%	2.285
Multilayered Nanofibrous Scaffold (MNS)	74.6%	2.513

angiogenesis, fibroblast proliferation, and remodelling of wounds.[39] HS is particularly known to be beneficial in chronic wound healing due to its anti-inflammatory activity as diabetes delays the wound healing process *via* a prolonged inflamma-

tory response.[40] Treatment with an anti-inflammatory agent can also help to advance into the cell proliferation and remodelling stages. In addition, TPGS-1000 might have provided additional benefits owing to its free radical scavenging activity, thereby promoting wound healing.[41] A research study by Li *et al.* proved the *in vivo* effectiveness of TPGS-1000 in promoting wound healing by increasing collagen accumulation and suppressing the inflammatory response at the wound site.[42] In addition, TPGS-1000 is known to promote fibroblast cell adhesion and proliferation.[43]

Histological studies conducted using Haematoxylin-Eosin (H&E) stain revealed the significant impact of nanofibers in wound healing (Fig. 5C). The nanofiber formulation treated
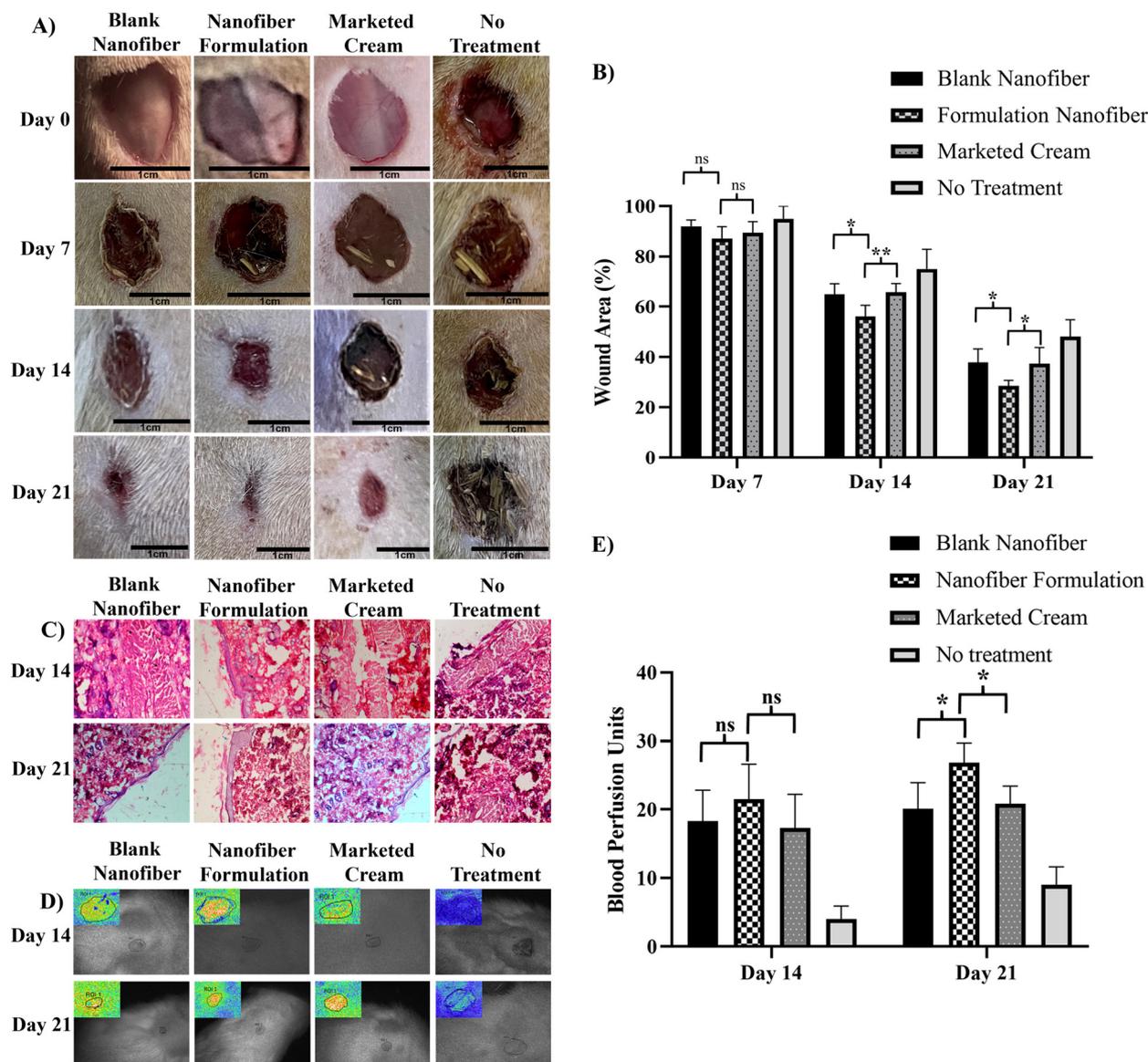

Fig. 5 (A) Digital images of the wound area of different animal groups. (B) Plot of the wound area and different time points. Two-way ANOVA was performed. Statistical differences are indicated as $*p < 0.05$ and $**p < 0.01$. (C) Microscopic images of tissue sections of different groups on day 14 and day 21. (D) Representative images of wound areas of different animal groups by laser Doppler flowmetry on day 14 and day 21 and (E) plot of BPU at different time points for different animal groups. Two-way ANOVA was performed. Statistical differences are indicated as $*p < 0.05$.

Table 3 Summary of histological analysis of healed tissue of different groups

Sample		Epithelialisation	Inflammation
Day 14	Blank nanofiber	No	Severe
	Nanofiber formulation	Yes	Mild
	Marketed cream	No	Moderate
	No treatment	No	Severe
Day 21	Blank nanofiber	Yes	Moderate
	Nanofiber formulation	Yes	Mild
	Marketed cream	Yes	Mild
	No treatment	No	Severe

group showed a marked difference in the presence of inflammatory cells compared to blank nanofibers and the control at day 14 and day 21. HS and TPGS-1000, owing to HS's anti-inflammatory and anti-oxidant properties, helped in reducing the exaggerated inflammatory response at the wound site. The nanofibers treated group showed re-epithelialisation at day 14 while the blank nanofiber and marketed cream treated groups showed re-epithelialisation only at day 21. The control group did not show any signs of re-epithelialisation even at day 21. Thus, the nanofiber formulation treated group showed a significant reduction in the inflammatory cells and effective re-epithelialisation at wound site (Table 3). The controlled inflammatory response and faster reepithelialisation provided by nanofibers were responsible for accelerated wound closure. Heparin and related molecules have also been reported to electrostatically interact and inhibit the activity of inflammatory cells secreted enzymes such as cathepsin G, proteinases, elastases, etc., which may degrade ECM and growth factors.[44,45]

Laser Doppler flowmetry was carried on day 14 and day 21 to measure the blood flow at the wound area in terms of blood perfusion units (BPU), as shown in Fig. 5D and E. There was no statistically significant difference in BPU between the groups on day 7. However, a significant ($p < 0.05$) improvement in the blood flow was observed on day 21 in the nanofiber formulation treated group compared to the blank nanofibers and marketed cream. The improved blood flow could be due to the role of HS in stabilizing and increasing local growth factor concentration and limiting endogenous growth factors degradation.[21] A higher blood flow to the wound tissue ensured a sufficient supply of nutrients to the wounded area and efficient removal of waste generated at the wound site. This may have favoured the wound healing study and thus could have significant effect in healing of chronic diabetic wound.

4. Conclusions

The present research work deals with the fabrication of multi-layered nanofibers of gelatin–PCL and TPGS-1000 loaded with HS via a layer-by-layer technique. Its activity of accelerating healing of diabetic wounds was confirmed in a rat model. The blend electrospinning requires the drug and polymer to be solubilized in a solvent system with good conductivity and low surface tension. The problem associated with HS is its solubility, which is only in water/water-based solvent systems. Hence, a mixture of acetic acid : water : ethyl acetate (4 : 4 : 2 v/v/v) was used for electrospinning of HS loaded gelatin–TPGS nanofibers. Further, the concentration of gelatin had a direct impact on the viscosity, conductivity, and spinnability of the solution as well as the morphology of the final nanofiber formulation. A good encapsulation efficiency of HS (89.2 ± 2.1%) was obtained. There were no structural changes in HS after electrospinning as confirmed by FTIR and PXRD studies. Gelatin being very hydrophilic in nature does not slow down the release of the entrapped drug. The additional layers of the PCL : gelatin solution of different ratios and thickness via layer-by-layer technique was able to sustain the drug release for up to 24 hours (F9 formulation). The wound healing study of the developed nanofiber formulation in diabetic rat models showed significant improvement in the wound closure rate compared to the marketed formulation treated group. The anti-inflammatory and neovascularization effects were assessed through histological and laser-Doppler flowmetry studies. Overall, this study demonstrated the possibility of blend electrospinning of highly water-soluble HS with gelatin using a water-based solvent system. The effect of additional layers of PCL–gelatin nanofibers on drug release was studied and the wound healing activity was confirmed in a diabetic animal model. In future, work should be undertaken to explore the utility of the reported method to encapsulate other similar drugs in gelatin-based nanofiber scaffolds and harness the complete potential of nanofibers for wound healing applications.

Abbreviations

MNS	Multilayered nanofibrous scaffold
HS	Heparin sodium
PCL	Poly-(ε-caprolactone)
GL	Gelatin
TPGS-1000	Tocopherol polyethylene glycol succinate-1000
DFU	Diabetic foot ulcer
ECM	Extracellular matrix
FTIR	Fourier transform infra-red
SEM	Scanning electron microscopy
DPPH	Diphenyl-1-picrylhydrazyl

Author contributions

Madhukiran R. Dhondale: Conceptualization, methodology, investigation, visualization, writing – original draft. Manjit Manjit: Methodology, investigation, data curation. Abhishek Jha: Methodology, investigation, formal analysis, writing – review & editing. Manish Kumar: Investigation, writing – review & editing. Kanchan Bharti: Formal analysis, investi-

gation. Dinesh Kumar: Writing – review & editing. Brahmeshwar Mishra: Supervision, conceptualization, resources, interpretation, writing – review & editing.

Data availability

The data supporting the findings of this study are available within the paper. Additional data shall be made available to the readers upon reasonable request.

Conflicts of interest

There are no conflicts to declare.

Acknowledgements

References

1 H. Brem and M. Tomic-Canic, Cellular and molecular basis of wound healing in diabetes, *J. Clin. Invest.*, 2007, **117**(5), 1219–1222.

2 Y. Song, Q. Hu, S. Liu, Y. Wang, H. Zhang, J. Chen and G. Yao, Electrospinning/3D printing drug-loaded antibacterial polycaprolactone nanofiber/sodium alginate-gelatin hydrogel bilayer scaffold for skin wound repair, *Int. J. Biol. Macromol.*, 2024, **275**, 129705.

3 G. Ajmal, G. V. Bonde, S. Thokala, P. Mittal, G. Khan, J. Singh, V. K. Pandey and B. Mishra, Ciprofloxacin HCl and quercetin functionalized electrospun nanofiber membrane: fabrication and its evaluation in full thickness wound healing, *Artif. Cells, Nanomed., Biotechnol.*, 2019, **47**(1), 228–240.

4 A. Li, L. Li, B. A. Zhao, X. Li, W. Liang, M. Lang, B. Cheng and J. Li, Antibacterial, antioxidant and anti-inflammatory PLCL/gelatin nanofiber membranes to promote wound healing, *Int. J. Biol. Macromol.*, 2022, **194**, 914–923.

5 I. Sebe, P. Szabó, B. Kállai-Szabó and R. Zelkó, Incorporating small molecules or biologics into nanofibers for optimized drug release: A review, *Int. J. Pharm.*, 2015, **494**(1), 516–530.

6 H. Duan, H. Chen, C. Qi, F. Lv, J. Wang, Y. Liu, Z. Liu and Y. Liu, A novel electrospun nanofiber system with PEGylated paclitaxel nanocrystals enhancing the transmucus permeability and in situ retention for an efficient cervicovaginal cancer therapy, *Int. J. Pharm.*, 2024, **650**, 123660.

7 M. Manjit, M. Kumar, K. Kumar, M. R. Dhondale, A. Jha, K. Bharti, Z. Rain, P. Prakash and B. Mishra, Fabrication of Dual Drug-Loaded Polycaprolactone–Gelatin Composite Nanofibers for Full Thickness Diabetic Wound Healing, *Ther. Delivery*, 2024, **15**(1), 5–21.

8 S. Chen, J. Zhou, B. Fang, Y. Ying, D.-G. Yu and H. He, Three EHDA Processes from a Detachable Spinneret for Fabricating Drug Fast Dissolution Composites, *Macromol. Mater. Eng.*, 2024, **309**(4), 2300361.

9 C. Huang, M. Wang, S. Yu, D.-G. Yu and S. W. Bligh, Electrospun Fenoprofen/Polycaprolactone @ Tranexamic Acid/Hydroxyapatite Nanofibers as Orthopedic Hemostasis Dressings, *Nanomaterials*, 2024, **14**(7), 646.

10 J. Zhou, T. Yi, Z. Zhang, D.-G. Yu, P. Liu, L. Wang and Y. Zhu, Electrospun Janus core (ethyl cellulose//polyethylene oxide) @ shell (hydroxypropyl methyl cellulose acetate succinate) hybrids for an enhanced colon-targeted prolonged drug absorbance, *Adv. Compos. Hybrid Mater.*, 2023, **6**(6), 189.

11 P. Zhao, K. Zhou, Y. Xia, C. Qian, D.-G. Yu, Y. Xie and Y. Liao, Electrospun trilayer eccentric Janus nanofibers for a combined treatment of periodontitis, *Adv. Fiber Mater.*, 2024, **6**(4), 1053–1073.

12 J. Zhou, Y. Chen, Y. Liu, T. Huang, J. Xing, R. Ge and D.-G. Yu, Electrospun medicated gelatin/polycaprolactone Janus fibers for photothermal-chem combined therapy of liver cancer, *Int. J. Biol. Macromol.*, 2024, **269**, 132113.

13 M. Wang, J. Hou, D.-G. Yu, S. Li, J. Zhu and Z. Chen, Electrospun tri-layer nanodepots for sustained release of acyclovir, *J. Alloys Compd.*, 2020, **846**, 156471.

14 D.-G. Yu, W. Gong, J. Zhou, Y. Liu, Y. Zhu and X. Lu, Engineered shapes using electrohydrodynamic atomization for an improved drug delivery, *WIREs Nanomed. Nanobiotechnol.*, 2024, **16**(3), e1964.

15 Y. Liu, X. Chen, X. Lin, J. Yan, D.-G. Yu, P. Liu and H. Yang, Electrospun multi-chamber core–shell nanofibers and their controlled release behaviors: A review, *WIREs Nanomed. Nanobiotechnol.*, 2024, **16**(2), e1954.

16 X. Huang, W. Jiang, J. Zhou, D.-G. Yu and H. Liu, The Applications of Ferulic-Acid-Loaded Fibrous Films for Fruit Preservation, *Polymers*, 2022, **14**(22), 4947.

17 B. D. Ulery, L. S. Nair and C. T. Laurencin, Biomedical applications of biodegradable polymers, *J. Polym. Sci., Part B: Polym. Phys.*, 2011, **49**(12), 832–864.

18 V. Guarino, G. Gentile, L. Sorrentino and L. Ambrosio, Polycaprolactone: Synthesis, Properties, and Applications, in *Encyclopedia of Polymer Science and Technology*, 2017, pp. 1–36.

19 D. R. Madhukiran, A. Jha, M. Kumar, G. Ajmal, G. V. Bonde and B. Mishra, Electrospun nanofiber-based drug delivery platform: advances in diabetic foot ulcer management, *Expert Opin. Drug Delivery*, 2021, **18**(1), 25–42.

20 M. Kumar, A. Jha and B. Mishra, Marine Biopolymers for Transdermal Drug Delivery, in *Marine Biomaterials: Drug Delivery and Therapeutic Applications*, ed. S. Jana and S.

Jana, Springer Nature Singapore, Singapore, 2022, pp. 157–207.

21 G. Kratz, C. Arnander, J. Swedenborg, M. Back, C. Falk, I. Gouda and O. Larm, Heparin-Chitosan Complexes Stimulate Wound Healing in Human Skin, *Scand. J. Plast. Reconstr. Surg. Hand Surg.*, 1997, **31**(2), 119–123.

22 M. Rullan, L. Cerdà, G. Frontera, L. Masmiquel and J. Llobera, Treatment of chronic diabetic foot ulcers with bemiparin: a randomized, triple-blind, placebo-controlled, clinical trial, *Diabetic Med.*, 2008, **25**(9), 1090–1095.

23 M. Kalani, J. Apelqvist, M. Blombäck, K. Brismar, B. R. Eliasson, J. W. Eriksson, B. Fagrell, A. Hamsten, O. Torffvit and G. Jörneskog, Effect of Dalteparin on Healing of Chronic Foot Ulcers in Diabetic Patients With Peripheral Arterial Occlusive Disease : A prospective, randomized, double-blind, placebo-controlled study, *Diabetes Care*, 2003, **26**(9), 2575–2580.

24 C. Page, Heparin and Related Drugs: Beyond Anticoagulant Activity, *ISRN Pharmacol.*, 2013, **2013**, 910743.

25 J. Jia, Structure and functions of heparan sulfate/heparin–Importance of glucuronyl C5-epimerase and heparanase, *Acta Univ. Ups.*, 2009, 46, https://www.diva-portal.org/smash/record.jsf?pid=diva2%3A228301&dswid=-2047.

26 S. Barrientos, O. Stojadinovic, M. S. Golinko, H. Brem and M. Tomic-Canic, PERSPECTIVE ARTICLE: Growth factors and cytokines in wound healing, *Wound Repair Regener.*, 2008, **16**(5), 585–601.

27 P. Olczyk, K. Komosińska-Vassev, K. Winsz-Szczotka, E. M. Koźma, G. Wisowski, J. Stojko, K. Klimek and K. Olczyk, Propolis modulates vitronectin, laminin, and heparan sulfate/heparin expression during experimental burn healing, *J. Zhejiang Univ., Sci., B*, 2012, **13**(11), 932–941.

28 R. Nirmala, B. Woo-il, R. Navamathavan, D. Kalpana, Y. S. Lee and H. Y. Kim, Influence of antimicrobial additives on the formation of rosin nanofibers via electrospinning, *Colloids Surf., B*, 2013, **104**, 262–267.

29 T. Liu, Y. Liu, Y. Chen, S. Liu, M. F. Maitz, X. Wang, K. Zhang, J. Wang, Y. Wang, J. Chen and N. Huang, Immobilization of heparin/poly-l-lysine nanoparticles on dopamine-coated surface to create a heparin density gradient for selective direction of platelet and vascular cells behavior, *Acta Biomater.*, 2014, **10**(5), 1940–1954.

30 B. Senturk, S. Mercan, T. Delibasi, M. O. Guler and A. B. Tekinay, Angiogenic Peptide Nanofibers Improve Wound Healing in STZ-Induced Diabetic Rats, *ACS Biomater. Sci. Eng.*, 2016, **2**(7), 1180–1189.

31 J.-H. Song, H.-E. Kim and H.-W. Kim, Production of electrospun gelatin nanofiber by water-based co-solvent approach, *J. Mater. Sci.: Mater. Med.*, 2008, **19**(1), 95–102.

32 Y. Li, J. Zhu, H. Cheng, G. Li, H. Cho, M. Jiang, Q. Gao and X. Zhang, Developments of Advanced Electrospinning Techniques: A Critical Review, *Adv. Mater. Technol.*, 2021, **6**(11), 2100410.

33 E.-R. Kenawy, M. S. A. El-Moaty, M. Ghoneum, H. M. A. Soliman, A. A. El-Shanshory and S. Shendy, Biobran-loaded core/shell nanofibrous scaffold: a promising wound dressing candidate, *RSC Adv.*, 2024, **14**(7), 4930–4945.

34 E. J. Chong, T. T. Phan, I. J. Lim, Y. Z. Zhang, B. H. Bay, S. Ramakrishna and C. T. Lim, Evaluation of electrospun PCL/gelatin nanofibrous scaffold for wound healing and layered dermal reconstitution, *Acta Biomater.*, 2007, **3**(3), 321–330.

35 G. Ajmal, G. V. Bonde, P. Mittal, G. Khan, V. K. Pandey, B. V. Bakade and B. Mishra, Biomimetic PCL-gelatin based nanofibers loaded with ciprofloxacin hydrochloride and quercetin: A potential antibacterial and anti-oxidant dressing material for accelerated healing of a full thickness wound, *Int. J. Pharm.*, 2019, **567**, 118480.

36 P. Wang, Y. Li, C. Zhang, F. Feng and H. Zhang, Sequential electrospinning of multilayer ethylcellulose/gelatin/ethylcellulose nanofibrous film for sustained release of curcumin, *Food Chem.*, 2020, **308**, 125599.

37 X. Sheng, L. Fan, C. He, K. Zhang, X. Mo and H. Wang, Vitamin E-loaded silk fibroin nanofibrous mats fabricated by green process for skin care application, *Int. J. Biol. Macromol.*, 2013, **56**, 49–56.

38 Z. Moazzami Goudarzi, T. Behzad, L. Ghasemi-Mobarakeh, M. Kharaziha and M. S. Enayati, Structural and mechanical properties of fibrous poly (caprolactone)/gelatin nanocomposite incorporated with cellulose nanofibers, *Polym. Bull.*, 2020, **77**(2), 717–740.

39 P. Olczyk, Ł. Mencner and K. Komosinska-Vassev, Diverse Roles of Heparan Sulfate and Heparin in Wound Repair, *BioMed Res. Int.*, 2015, **2015**, 549417.

40 M. Oremus, M. Hanson, R. Whitlock, E. Young, A. Gupta, A. Dal Cin, C. Archer and P. Raina, The uses of heparin to treat burn injury, *Evidence Rep. Technol. Assess. (Full Rep.)*, 2006, (148), 1–58.

41 P. Leme Goto, M. Cinato, F. Merachli, B. Vons, T. Jimenez, D. Marsal, N. Todua, H. Loi, Y. Santin, S. Cassel, M. Blanzat, H. Tronchere, C. Dejugnat, O. Kunduzova and F. Boal, In vitro and in vivo cardioprotective and metabolic efficacy of vitamin E TPGS/Apelin, *J. Mol. Cell. Cardiol.*, 2020, **138**, 165–174.

42 H. Li, M. Wang, G. R. Williams, J. Wu, X. Sun, Y. Lv and L.-M. Zhu, Electrospun gelatin nanofibers loaded with vitamins A and E as antibacterial wound dressing materials, *RSC Adv.*, 2016, **6**(55), 50267–50277.

43 S. A. Kheradvar, J. Nourmohammadi, H. Tabesh and B. Bagheri, Starch nanoparticle as a vitamin E-TPGS carrier loaded in silk fibroin-poly(vinyl alcohol)-Aloe vera nanofibrous dressing, *Colloids Surf., B*, 2018, **166**, 9–16.

44 P. V. Peplow, Glycosaminoglycan: a candidate to stimulate the repair of chronic wounds, *Thromb. Haemostasis*, 2005, **94**(07), 4–16.

45 J. Wang, H. Zheng, X. Qiu, A. Kulkarni, L. M. Fink and M. Hauer-Jensen, Modulation of the intestinal response to ionizing radiation by anticoagulant and non-anticoagulant heparins, *Thromb. Haemostasis*, 2005, **94**(11), 1054–1059.